Magnetic order and crystal field excitations in $Er_2Ru_2O_7$: a neutron scattering study

2009 J. Phys.: Condens. Matter 21 436004

(http://iopscience.iop.org/0953-8984/21/43/436004)

J. Phys.: Condens. Matter **21** (2009) 436004 (6pp) doi:10.1088/0953-8984/21/43/436004

Magnetic order and crystal field excitations in $Er_2Ru_2O_7$: a neutron scattering study

J S Gardner[1,2] **and G Ehlers**[3]

[1] Department of Physics, Indiana University, Bloomington, IN 47408, USA
[2] NCNR, NIST, Gaithersburg, MD 20899-6102, USA
[3] SNS, Oak Ridge National Laboratory, Oak Ridge, TN 37831-6475, USA

E-mail: jsg@nist.gov

Received 18 August 2009, in final form 13 September 2009
Published 8 October 2009
Online at stacks.iop.org/JPhysCM/21/436004

Abstract
The magnetic pyrochlore $Er_2Ru_2O_7$ has been studied with neutron scattering and susceptibility measurements down to a base temperature of 270 mK. For the low temperature phase in which the Er sublattice orders, new magnetic Bragg peaks are reported which can be indexed with integer (hkl) for a face centered cubic cell. Inelastic measurements reveal a wealth of crystal field levels of the Er ion and a copious amount of magnetic scattering below 15 meV. The three lowest groups of crystal field levels are at 6.7, 9.1 and 18.5 meV.

(Some figures in this article are in colour only in the electronic version)

1. Introduction

Over the past 20 years, oxides with the cubic pyrochlore structure have attracted a great deal of attention because they display a rich variety of unusual magnetic phenomena at low temperatures, which are related to the effects of geometric frustration. This term refers to the inability of a system, by geometric arrangement of the magnetic ions, to minimize all pairwise interactions simultaneously. In condensed matter magnetism, frustration may result in the absence of magnetic order, spin-glass or spin-liquid behavior, or the development of exotic magnetic phases [1]. However, frustration is found in other areas of condensed matter physics as well. It arises in liquid crystals, in superconducting Josephson junction arrays in a magnetic field and in protein folding [2].

The pyrochlore oxides, with space group $Fd\bar{3}m$ (no. 227), have eight formula units of the general formula $A_2B_2O_7$ in one unit cell [3]. The A and B atoms individually form three-dimensional networks of corner-sharing tetrahedra, which are displaced by a $(\frac{1}{2}\frac{1}{2}\frac{1}{2})$ vector. Most pyrochlores studied to date for their magnetic properties have a trivalent rare-earth on the A site and a tetravalent metal ion on the B site. For practical reasons, most studies have been carried out on pyrochlores where only the A lattice is magnetic. These systems are not complicated by A–B magnetic interactions and the rare-earth moments are typically large [4]. Of particular interest are the titanates ($A_2Ti_2O_7$), mainly because large single crystals are available [5, 6]. These studies have included $Tb_2Ti_2O_7$, a spin liquid [7], an order-by-disorder transition in $Er_2Ti_2O_7$ [8], a phase transition between dynamic states in $Yb_2Ti_2O_7$ [9] and the spin ices $Ho_2Ti_2O_7$ and $Dy_2Ti_2O_7$ [10, 11]. A few compounds, in which the B site possesses the only magnetic ion, have also been studied. Examples include $Y_2Mo_2O_7$, a spin glass with very little structural disorder [12], $Y_2Ru_2O_7$ with a huge Curie temperature of 1100 K [13], in which magnetic order sets in only at 95 K, and the superconductor $Cd_2Re_2O_7$ [14].

The systems tend to get much more complicated when both the A and B sites are occupied by magnetic ions. Not only does frustration affect each individual sublattice differently, but also the magnetic interactions between the 4f electrons of the rare-earth ions and the d electrons on the B site add to the problem. It should be noted here that the A–A, B–B and A–B bond distances are equal in the face centered cubic lattice. The ordered spin ice, $Ho_2Ru_2O_7$ [15], a disorder-free spin glass, $Tb_2Mo_2O_7$ [16], and $Nd_2Mo_2O_7$ [17] showing an anomalous Hall effect are examples of such pyrochlore compounds studied to date.

Very little is known about the magnetic properties of ruthenate pyrochlores [18–23], although ruthenates have

been studied extensively in other structural forms like the perovskite [24, 25] and layered perovskite structures [26–28]. Recently, there has been some interest in the spin glass $Ca_2Ru_2O_7$, with its spin-1/2, Ru^{5+} network of corner-sharing tetrahedra [29]. In the rare-earth ruthenates ($A_2Ru_2O_7$) the small magnetic moment (≈1–2 μ_B) associated with the Ru^{4+} ion ($S = 1$) has been shown to order at relatively high temperature, between ≈70 and 160 K, depending on the ionic size of the rare-earth ion [20, 21]. Long-range magnetic correlations between the rare-earth ions are expected to develop only at temperatures below 2 K, but very little bulk data (such as magnetic susceptibility) have been published in this temperature range. Perhaps the best studied ruthenate pyrochlore is $Ho_2Ru_2O_7$, which has many bulk properties similar to the known spin-ice compounds [15, 30, 31]. Unlike a spin ice, the Ho^{3+} sublattice orders at 1.4 K [30], but the ordering pattern is very similar to the short-range order seen in the spin ices. Each magnetic moment is slightly tilted from the local easy axis, creating a long-range-ordered canted ferromagnet. Wiebe *et al* [30], also reported some unusual observations: (i) the magnetic Bragg peaks associated with the ruthenium ordering were not resolution-limited; rather, a correlation length of over ≈200 Å (or ≈20 unit cells) was found and (ii) it was also shown that the ordering of the Ru sublattice affects the single-ion properties of Ho^{3+} to some extent by modifying the energies of some of the crystal field levels.

In this paper we report on the magnetic properties of $Er_2Ru_2O_7$, in order to understand further the interplay between d and f electrons in this double-pyrochlore compound. Bulk property measurements have previously shown the Ru sublattice to order at ∼92 K [20], whilst the Er sublattice remains dynamic down to 5 K [21]. In a subsequent neutron diffraction study it was found that both sublattices possess frozen, long-range magnetic correlations at 3 K [23]. At this temperature the magnetic and structural unit cells are of the same size, with the Er and Ru magnetic moments antiferromagnetically oriented toward the same (a global) [100] direction.

2. Experimental details

A 10 g polycrystalline sample was prepared by the conventional solid-state reaction at the NIST Center for Neutron Research. High purity (>99.99%) erbium sesquioxide Er_2O_3 and ruthenium dioxide RuO_2 were used as starting materials. These were weighed in the correct metal ratio and then 3% RuO_2 was added to account for its high volatility. The well-mixed powders were heated at 1150 °C for 8 h, reground and heated again at 1200 °C for another 12 h. Room temperature x-ray powder diffraction (using Cu Kα radiation) revealed that the sample was single phase with a cubic lattice parameter of 10.11(1) Å.

Neutron scattering experiments were performed at the new Cold Neutron Chopper Spectrometer (CNCS) in Oak Ridge [32]. This instrument, at beamline 5 of the Spallation Neutron Source (SNS), is a direct geometry, multi-chopper inelastic spectrometer designed to perform best with incident neutron energies between 2 and 50 meV and to provide flexibility in the choice of the energy resolution. The sample was placed inside a He flow cryostat with a ^{3}He insert (capable of reaching a base temperature of 270 mK). Two settings for incident neutron energy were chosen, $E_i = 22$ meV to cover a broad range of (Q, ω) space, and $E_i = 5$ meV for better energy resolution. The resulting energy resolution (full width at half-maximum, FWHM) was 1.1 meV (at $E_i = 22$ meV) and 0.14 meV (at $E_i = 5$ meV), respectively. Control measurements of an empty sample container and a vanadium foil were used to correct the raw data.

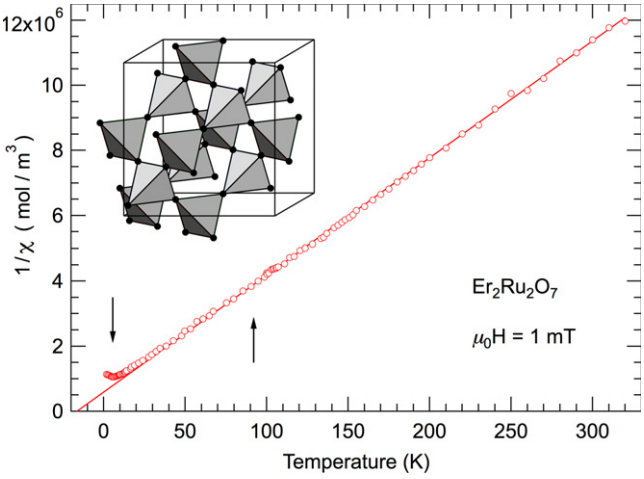

Figure 1. The inverse uniform magnetic susceptibility measured as a function of temperature in a field of 1 mT and the Curie–Weiss fit to the high temperature region extended to the temperature axis intercept. The arrows mark the two phase transition temperatures determined by specific heat. The inset shows the Er sublattice in the pyrochlore structure.

3. Results

A small amount (100 mg) of the sample was used for magnetization measurements. Figure 1 shows the temperature dependence of the inverse susceptibility measured with a SQUID magnetometer in a field of $\mu_0 H = 1$ mT. A fit of the high temperature regime (>200 K) to a Curie–Weiss law, $\chi^{-1} \sim T - \theta_{CW}$, yields an antiferromagnetic Curie–Weiss temperature of $\theta_{CW} = -16 \pm 5$ K and a paramagnetic moment of 9.2 μ_B. This value compares favorably with the free ion value appropriate for the $^4I_{15/2}$ Er^{3+} ion, which will dominate the paramagnetic bulk properties. As the temperature is lowered below 120 K, the data begins to deviate from the Curie–Weiss law as spin–spin correlations build up, particularly in the Ru^{4+} sublattice which orders at ∼92 K [20]. However, the inverse susceptibility continues to decrease as the temperature is lowered until 5.5 K when it abruptly turns up. This upturn in susceptibility is concomitant with the appearance of new magnetic Bragg peaks in neutron diffraction which are associated with the long-range ordering of the rare-earth sublattice [23].

Elastic neutron scattering data collected at CNCS at various temperatures is shown in figure 2, where the scattering

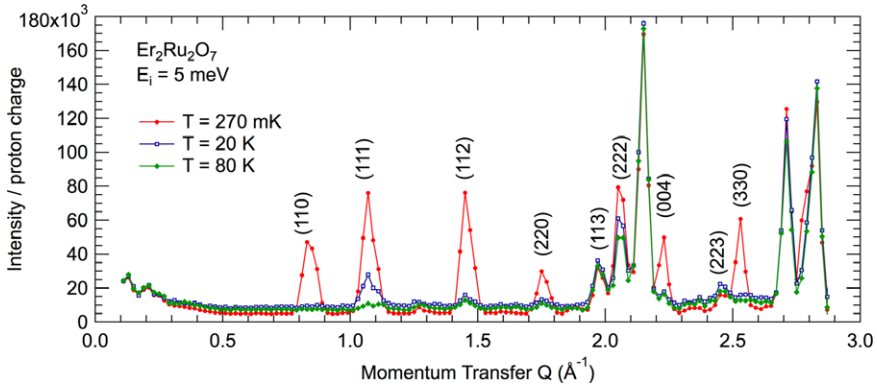

Figure 2. Neutron scattering data measured at CNCS ($E_i = 5$ meV) at various temperatures, integrated in the range ± 0.1 meV. Bragg peaks are indexed in the fcc cubic unit cell. Errors representing $\pm 1\sigma$ are smaller than the data points and the lines are guides to the eyes.

between ± 0.1 meV was summed up and plotted as a function of $|Q|$. At high temperature, only the peaks associated with the $Fd\bar{3}m$ chemical unit cell (and the sample environment) are observed. At 80 K, some additional intensity can be seen on top of the existing Bragg peaks, which is associated with the $Q = 0$, ordered structure of the Ru sublattice. As the system cools further this intensity grows, consistent with what was reported by Taira *et al* [23], since the Er sublattice is polarized by the ordered ruthenium. However, at base temperature new Bragg peaks occur, which were not previously reported, such as (110), (112), etc. These can still be indexed with a face centered cubic cell as shown in figure 2. Since the $|Q|$ range is rather limited, these data unfortunately do not allow us to identify the ordered magnetic phase, which will require a new dedicated low temperature neutron diffraction study.

Figure 2 also reveals a measurable amount of diffuse scattering at all temperatures above the Er ordering temperature. This is ubiquitous in rare-earth-based frustrated magnets, where strong, local spin–spin correlations develop at high temperature but reach beyond the nearest-neighbor distances only at considerably lower temperatures. Single-crystal [33, 34] or polarization analysis studies [35, 36] would allow one to investigate this scattering further and address the dynamics of the Er spins. At the temperatures studied this scattering is quite flat in $|Q|$, indicative of a lack of spatial correlations between the Er^{3+} magnetic moments.

Figure 3 summarizes the inelastic data collected between 270 mK and 150 K with 22 meV incident energy neutrons. Significant changes to the spectra can be seen as the temperature is changed. All major inelastic scattering features in figure 3 appear to be independent of Q, suggesting that in their paramagnetic phases the spins are poorly correlated and single-ion-like. Significantly, even as the system is cooled through the Er ordering temperature, no dispersion is seen over the entire $|Q|$ range.

Since these modes are dispersionless, one-dimensional cuts along the energy axis, integrating over the range 1 $\text{Å}^{-1} \leqslant |Q| \leqslant 6$ Å^{-1}, allow a better description of the data (see figure 4). This is a large integration range to reveal magnetic features in the scattering, but upon examining the high versus low Q data separately, no significant phonon contribution to the high Q data was found. From figure 4 it becomes clear that the spectrum is more complicated than one would first suspect from figure 3. It also becomes apparent that, on the neutron energy gain side (negative numbers), the instrumental energy resolution is less good and that some excitations seen as single broad lines (indicated by arrows) can, in fact, be resolved as pairs of modes.

At 150 K, gross features can be seen in the data at approximately 2.5, 6.7, 9.1, 12 and 18.5 meV. All these modes diminish in intensity as $|Q|$ increases and represent transitions between various crystalline electric field (CEF) levels. One can distinguish CEF transitions that involve the ground state from others that do not involve the ground state through their temperature dependence of the intensity. As higher energy states are increasingly populated at increasing temperature, transitions out of the ground state (neutron energy loss) will decrease monotonically in intensity as the experimental temperature increases. The three modes observed at 6.7, 9.1 and 18.5 meV and labeled 'A', 'B' and 'C' in figure 4 possess such a temperature dependence and are thus identified as transitions out of the ground state. These energies compare favorably with the first three excited states in $Er_2Ti_2O_7$ as will be discussed further below [37, 38]. In contrast, the temperature dependence of the lower energy mode at $\approx$2.5 meV suggests that this is not out of the ground state, and is more likely to be a transition between the modes at 6.7 and 9.1 meV. It becomes active between 20 and 80 K, which is consistent with requiring the level at 6.7 meV ($\sim$78 K) to be thermally populated.

The situation is complicated further in $Er_2Ru_2O_7$ due to the presence of a moment on the Ru site, resulting in a Zeeman splitting of the crystal field levels at all temperatures studied, and small energy shifts of some of the modes as the temperature is varied. For example, an additional mode is revealed in the 5 meV dataset at 1.5 meV (only in the 270 mK dataset on the neutron energy loss side). A hint of this can be seen in figure 4. This is probably a result of the Zeeman splitting of the ground-state doublet by the magnetic fields produced in the sample as the Er sublattice orders at 5.5 K.

Figure 4 reveals a considerable amount of magnetic spectral weight over a wide range in energy (0–15 meV) that clearly exists over the entire Q range covered by the

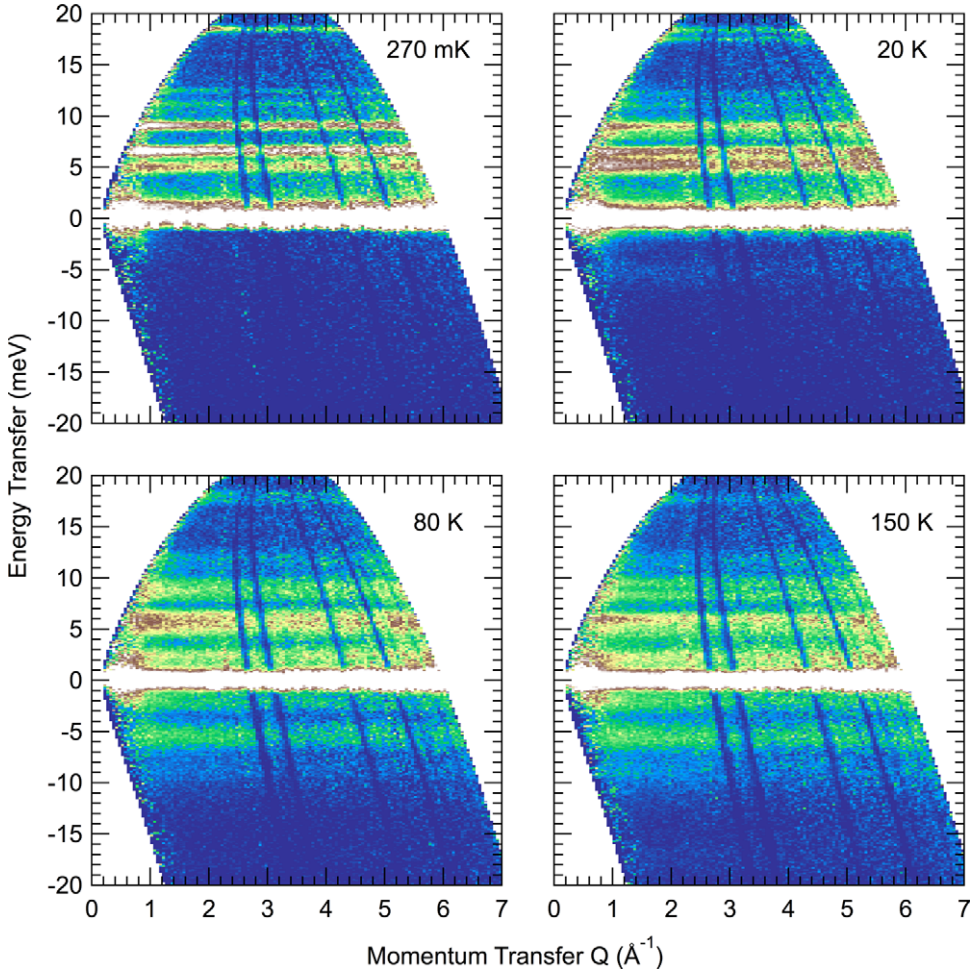

Figure 3. False color contour plots of the inelastic spectra from $Er_2Ru_2O_7$ in different magnetic phases. The vertical dark lines are due to an instrumental effect.

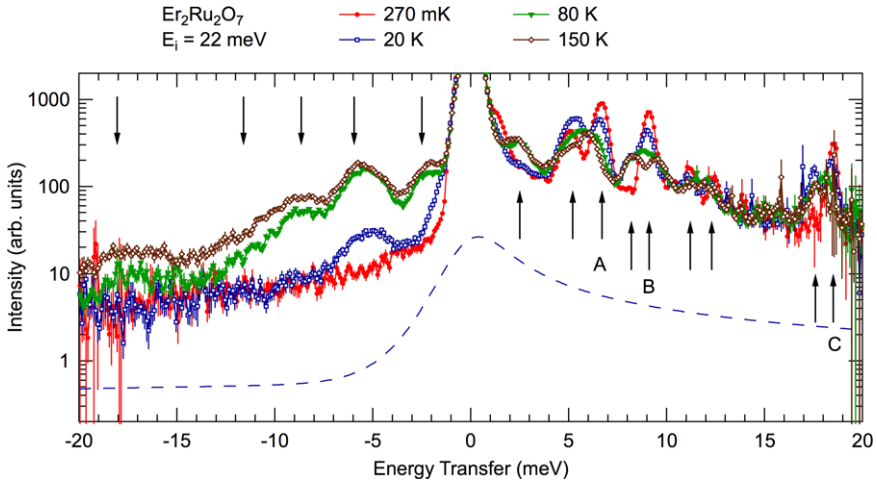

Figure 4. Spectra integrated over the range 1 Å^{-1} $\leqslant |Q| \leqslant$ 6 Å^{-1}. Transitions are marked by arrows (see text). The dashed line depicts the scattering one would observe for a single Lorentzian process with FWHM $\sim$ 3 meV at $T = 20$ K (offset by a constant factor for better visibility).

experiment (see figure 3). Similar spin dynamics were seen in $Y_2Ru_2O_7$ by van Duijn *et al* [13]. Without the added complication of the rare-earth moment, they were able to measure a gap opening up in the excitation spectrum below the Ru^{4+} ordering and estimated a spin relaxation rate. In $Er_2Ru_2O_7$, however, this is not observed, presumably due

to the presence of the magnetic moment of the A site. As indicated in figure 4 by the dashed line, the 'background' scattering can qualitatively be attributed to a single Lorentzian (i.e. not gapped) process which is weighted by the temperature-dependent Bose factor and convoluted with the instrumental resolution.

4. Discussion

Elastic scattering studies at 270 mK have revealed a new magnetic phase in $Er_2Ru_2O_7$. Previous neutron diffraction studies by Taira *et al* [23] reported the magnetic ordering of the Er sublattice at 10 K, at significantly higher temperatures than by bulk property measurements [21]. At 3 K they refined a collinear antiferromagnetic structure with about half the expected moment (4.5 μ_B) on the Er ion. In our studies we have performed elastic measurements at 270 mK, well below the ordering temperature suggested by bulk property measurements, and we found Bragg peaks associated with the true ordering of the Er sublattice that have never been reported before. We assume that the collinear ordering previously reported is a precursor to the true ordering of the Er ion, and a result of the spin polarization due to Er–Ru exchange interactions. At 20 K we see a similar phase, with significant magnetic scattering at (111), for example. We find that the Er sublattice orders into a $Q = 0$ type structure, where the magnetic unit cell is the same size as the chemical unit cell and the face centered cubic symmetry is conserved, but this study has insufficient data to conclude anything else.

In the trigonal geometry at the rare-earth site ($\bar{3}m$), and in the absence of a magnetic field, the 16-fold degenerate ground state of the free Er ion ($^4I_{15/2}$) splits into 8 Kramers doublets [37–39]. Three transitions, at 6.7, 9.1 and 18.5 meV (labeled 'A', 'B' and 'C') in figure 4, can be identified, through their temperature dependence, as transitions involving the ground state. These values compare favorably with the first three excited states in the isostructural $Er_2Ti_2O_7$. Dasgupta *et al* [37] calculated the crystal field Hamiltonian for $Er_2Ti_2O_7$ and found three crystal field energies below 20 meV (the dynamic range experimentally explored in this paper) at 6.4, 7.7 and 11.9 meV and 6 within the first 40 meV. Shirai [38] determined the first levels experimentally through neutron scattering at 6.4, 7.3 and 15.4 meV.

In $Er_2Ru_2O_7$, however, the situation is more complex due to the magnetic ordering of both the Ru and Er sublattices. An internal field, associated with large clusters of ordered spins, will alter the local environment of the rare-earth site which can result not only in an energy shift of the excitations, but also Zeeman splitting of the doublets. This is clearly seen in figure 3: as the system cools down, the scattering on the negative (neutron energy gain) side is reduced as expected because the CEF levels are not thermally populated to provide the neutron with additional energy. The positive (neutron energy loss) side reveals that the overall picture changes significantly with temperature, as some excitations sharpen up and some new levels appear. For example, cooling through the Ru ordering temperature (92 K) causes the mode at ≈6.3 meV to broaden. Upon cooling further this mode splits into two distinct excitations. In contrast, the levels at 9.1 and 18.5 meV are clearly single excitations at base temperature and split as the system warms up. To determine the complete crystal field Hamiltonian, other complementary probes like Mössbauer spectroscopy and light scattering are required along with more neutron studies, especially at temperatures greater than 150 K, to overcome the complications associated with the two magnetic species in this double-pyrochlore lattice compound.

Acknowledgments

The authors wish to thank C Adriano for help preparing and characterizing the sample and R A Mills, J L Niedziela and A A Podlesnyak for assistance during the neutron scattering experiment. This research at Oak Ridge National Laboratory's Spallation Neutron Source was sponsored by the Scientific User Facilities Division, Office of Basic Energy Sciences, US Department of Energy.

References

[1] Diep H T (ed) 1994 *Magnetic Systems with Competing Interactions* (Singapore: World Scientific)
Diep H T (ed) 2004 *Frustrated Spin Systems* (Singapore: World Scientific)
Gardner J S, Gingras M J P and Greedan J E 2009 arXiv:0906.3661
[2] Onuchic J N, Luthey-Schulten Z and Wolynes P G 1997 *Annu. Rev. Phys. Chem.* **48** 545
[3] Subramanian M A, Aravamudan G and Subba Rao G V 1983 *Prog. Solid State Chem.* **15** 55
[4] Greedan J E 2006 *J. Alloys Compounds* **408** 444
[5] Gardner J S, Gaulin B D and Paul D M 1998 *J. Cryst. Growth* **191** 740
[6] Balakrishnan G, Petrenko O A, Lees M R and Paul D M 1998 *J. Phys.: Condens. Matter* **10** L723
[7] Gardner J S *et al* 1999 *Phys. Rev. Lett.* **82** 1012
[8] Champion J D M *et al* 2003 *Phys. Rev.* B **68** 020401
[9] Hodges J A *et al* 2002 *Phys. Rev. Lett.* **88** 077204
[10] Bramwell S T and Gingras M J P 2001 *Science* **294** 1495
[11] Ehlers G, Mamontov E, Zamponi M, Kam K C and Gardner J S 2009 *Phys. Rev. Lett.* **102** 016405
[12] Gardner J S, Gaulin B D, Lee S-H, Broholm C, Raju N P and Greedan J E 1999 *Phys. Rev. Lett.* **83** 211
[13] van Duijn J, Hur N, Taylor J W, Qiu Y, Huang Q Z, Cheong S W, Broholm C and Perring T G 2008 *Phys. Rev.* B **77** 020405
[14] Sakai H, Yoshimura K, Ohno H, Kato H, Kambe S, Walstedt R E, Matsuda T D, Haga Y and Onuki T 2001 *J. Phys.: Condens. Matter* **13** L785
[15] Bansal C, Kawanaka H, Bando H and Nishihara Y 2002 *Phys. Rev.* B **66** 052406
[16] Greedan J E, Reimers J N, Penny S L and Stager C V 1990 *J. Appl. Phys.* **67** 5967
[17] Yoshii S, Iikubo S, Kageyama T, Oda K, Kondo Y, Murata K and Sato M 2000 *J. Phys. Soc. Japan* **69** 3777
[18] Taira N, Wakeshima M and Hinatsu Y 1999 *J. Solid State Chem.* **144** 216
[19] Ito M, Yasui Y, Kanada M, Harashina H, Yoshii S, Murata K, Sato M, Okumura H and Kakurai K 2000 *J. Phys. Soc. Japan* **69** 888
[20] Ito M, Yasui Y, Kanada M, Harashina H, Yoshii S, Murata K, Sato M, Okumura H and Kakurai K 2001 *J. Phys. Chem. Solids* **62** 337

[21] Taira N, Wakeshima M and Hinatsu Y 2002 *J. Mater. Chem.* **12** 1475
[22] Bansal C, Kawanaka H, Bando H and Nishihara Y 2003 *Physica* B **329–333** 1034
[23] Taira N, Wakeshima M, Hinatsu Y, Tobo A and Ohoyama K 2003 *J. Solid State Chem.* **176** 165
[24] Longo J M, Raccah P M and Goodenough J B 1968 *J. Appl. Phys.* **39** 1327
[25] Gardner J S, Balakrishnan G and Paul D M 1995 *Physica* C **252** 303
[26] Maeno Y, Hashimoto H, Yoshida K, Nishizaki S, Fujita T, Bednorz J G and Lichtenberg F 1994 *Nature* **372** 532
[27] Gardner J S, Balakrishnan G, Paul D M and Haworth C 1996 *Physica* C **265** 251
[28] Grigera S A, Perry R S, Schofield A J, Chiao M, Julian S R, Lonzarich G G, Ikeda S I, Maeno Y, Millis A J and Mackenzie A P 2001 *Science* **294** 329
[29] Munenaka T and Sato H 2006 *J. Phys. Soc. Japan* **75** 103801
Taniguchi T, Munenaka T and Sato H 2009 *J. Phys.: Conf. Ser.* **145** 012017
[30] Wiebe C R, Gardner J S, Kim S J, Luke G M, Wills A S, Gaulin B D, Greedan J E, Swainson I, Qiu Y and Jones C Y 2004 *Phys. Rev. Lett.* **93** 076403
[31] Gardner J S, Cornelius A L, Chang L J, Prager M, Brückel T and Ehlers G 2005 *J. Phys.: Condens. Matter* **17** 7089
[32] Mason T E *et al* 2006 *Physica* B **385/386** 955
and http://neutrons.ornl.gov/instrument_systems/beamline_05_cncs/index.shtml
[33] Gardner J S, Gaulin B D, Berlinsky A J, Waldron P, Dunsiger S R, Raju N P and Greedan J E 2001 *Phys. Rev.* B **64** 224416
[34] Bramwell S T *et al* 2001 *Phys. Rev. Lett.* **87** 047205
[35] Stewart J R, Ehlers G, Wills A S, Bramwell S T and Gardner J S 2004 *J. Phys.: Condens. Matter* **16** L321
[36] Rule K C *et al* 2007 *Phys. Rev.* B **67** 212405
[37] Dasgupta P, Jana Y and Ghosh D 2006 *Solid State Commun.* **139** 424
[38] Shirai M 2006 *Thesis* University College London
[39] Runciman W A 1956 *Phil. Mag.* **1** 1075